ASSESSMENT OF THE HEAT TRANSFER MODEL AND TURBULENT WALL FUNCTIONS FOR TWO FLUID CFD SIMULATIONS OF SUBCOOLED AND SATURATED BOILING

D. Prabhudharwadkar[1], M. Lopez de Bertodano[1], J. Buchanan Jr.[2]

[1]Purdue University, School of Nuclear Engineering, 400 Central Drive, West Lafayette, IN-47906, USA

[2]Bechtel Marine Propulsion Corporation, West Mifflin PA-15122, USA

Abstract

This paper describes the details of validation of the two-fluid model for boiling simulations using the CFD code CFX. In particular, since subcooled boiling occurs at a superheated wall placed in a subcooled liquid, most of the heat and mass transfer takes place close to the wall. Therefore, this study was focused on the assessment of two important aspects of near wall predictions, viz., the wall heat transfer model and the turbulent wall functions. Validation was performed using the state-of-the-art multidimensional experimental data available in the literature.

The first part is an assessment of the wall heat transfer model which is based on splitting the wall heat flux into three components, viz., the single phase convection, the evaporation at the bubble surface and the quenching effect at the heated wall after the bubble departure. The evaporation and quenching components use the following three closure parameters: 1. Bubble Nucleation Site Density, 2. Bubble Departure Diameter, and 3. Bubble Departure Frequency. Data sets where the bubble diameter has been measured have been selected to eliminate one unknown so the assessment is limited to the nucleation site density and the departure frequency correlations available in the open literature.

The second part of the paper is an assessment of the turbulent wall functions used to prescribe the wall boundary conditions for momentum and turbulence quantities and hence influence the near wall velocity and turbulence distribution. The state-of-the-art two-fluid model uses a two-phase k-ε turbulence model (Lopez de Bertodano et al., 1994) with the standard logarithmic wall function (Launder and Spalding, 1974). Although the law-of-the-wall is universal for single phase flows, the same is not true when the boundary layer contains a two-phase bubbly mixture. Previous experiments (Marie et al., 1997) have shown that the velocity profile still follows a logarithmic profile but the slope and the intercept constant vary with the concentration of bubbles and the relative magnitude of the shear and buoyant forces. A modification of the law of the wall coefficients has been suggested by Marie et al. (1997) based on the experimental data obtained from adiabatic air-water bubbly flow over a vertical flat plate. The wall law coefficients of CFX were modified using the two-phase wall function model and significant improvements were noticed in the turbulent parameter predictions.

NOMENCLATURE

a_i	Interfacial Area Concentration
C_D	Drag Coefficient
C_{VM}	Coefficient of Virtual Mass (0.5)
D_b	Bubble Diameter
D_{dep}	Bubble departure diameter
e_k	Phase enthalpy
f_{dep}	Bubble departure frequency
g	Gravitational Acceleration
h_{lg}	Latent heat of evaporation
j_L	Superficial Velocity of Liquid
j_G	Superficial Velocity of Gas
k	Turbulence Kinetic Energy
$\underline{M}_{ki}$	Interfacial Momentum Source
Δm_k	Mass Source
n_{site}	Nucleation site density
q''	Heat Flux
$\underline{\overline{v}}_k$	Velocity (vector)
$\underline{\overline{v}}_R$	Relative Velocity (vector)
T	Temperature

Greek Symbols

α_k	Volume Fraction of k^{th} phase
α	Void Fraction
ε	Dissipation of Turbulence Kinetic Energy
ρ_k	Density
$\underline{\underline{\tau}}_k^{Re}$	Turbulent (Reynolds) Stress
μ	Dynamic viscosity

λ	Thermal Conductivity

Superscript

D	Drag
TD	Turbulent Diffusion
L	Lift
W	Wall

Subscript

k	Phase identifier
1, l, f, L	Continuous (Liquid) Phase
2, g, G	Dispersed (Gas) Phase
dep	Departure
t	Turbulent

1. INTRODUCTION

The prediction of boiling flows depends on accurate representation of the heat and mass transfer processes at the wall where the vapor is formed. The accuracy of the model prediction depends on how well the following three independent parameters are estimated: 1. Bubble Nucleation Site Density, 2. Bubble Departure Diameter, and 3. Bubble Departure Frequency. These parameters depend on complex physical phenomena that are not completely understood. Different closure relations exist in the literature for each of the above parameters which are discussed in detail in the next section.

One of the goals of the present study is to perform an independent assessment of each of these parameters from the perspective of CFD implementation. However, it is difficult to test three separate uncertainties simultaneously and hence only those data sets have been selected where the bubble diameter has been measured. A review of the departure frequency models was done to select the one best suited for the present data sets. Then, using the known departure bubble size and the chosen departure frequency model, two well known models for the nucleation site density were implemented and the results were compared.

The heat transfer at the wall also depends on the turbulence intensity near the wall and this should be correctly predicted as well. The wall function approach that is usually used with the Standard k-epsilon model to obtain the near wall turbulence quantities using coarser meshes needs a correction that accounts for the effect of presence of a two-phase mixture. Such an approach has been implemented successfully for adiabatic flows (Marie et al., 1997) and this has been extended for boiling flows here.

The two-fluid model used here was previously tested for adiabatic flows where the interfacial momentum transfer terms were validated (Prabhudharwadkar et al., 2009). The energy equation along with the interfacial heat and mass transfer correlations were incorporated into the model. The next section describes in detail the two-fluid model used in this study.

2. TWO-FLUID MODEL WITH HEAT AND MASS TRANSFER

For *diabatic* flows, the ensemble averaged two-fluid model equations (Ishii and Hibiki, 2006) governing the motion of each phase has the following form:

Mass Conservation:

$$\frac{\partial}{\partial t}\alpha_k \rho_k + \nabla\cdot\alpha_k \rho_k \underline{\overline{v}}_k = \Delta m_k \tag{1}$$

Momentum conservation:

$$\frac{\partial}{\partial t}\alpha_k \rho_k \underline{\overline{v}}_k + \nabla\cdot\alpha_k \rho_k \underline{\overline{v}}_k \underline{\overline{v}}_k = -\alpha_k \nabla p_k + \nabla\cdot\alpha_k\left(\underline{\underline{\tau}}_k + \underline{\underline{\tau}}_k^{\mathrm{Re}}\right) + \alpha_k \rho_k \underline{g} + \underline{M}_{ki} + \sum_j \Delta m_{k,j}\underline{\overline{v}}_j \tag{2}$$

Energy conservation:

$$\frac{\partial}{\partial t}\alpha_k \rho_k e_k + \nabla\cdot\alpha_k \rho_k \underline{\overline{v}}_k e_k = -\nabla\cdot\left[\alpha_k\left(\underline{q}_k'' + \underline{q}_k''^{\mathrm{Re}}\right)\right] - p\left[\frac{\partial \alpha_k}{\partial t} + \nabla\cdot\left(\alpha_k \underline{\overline{v}}_k\right)\right] + \Delta m_k H_{ki} + q_{ki} \tag{3}$$

$$\underline{q}_k'' = -\lambda_k \nabla T_k\,,\quad \underline{q}_k''^{\mathrm{Re}} = -\frac{\rho_k \nu_{tk}}{\mathrm{Pr}_t}\nabla e_k \tag{4}$$

In the present calculations of subcooled boiling, the vapor generated was assumed to be at saturated temperature and hence was treated as isothermal phase.

2.1 Interfacial momentum transfer

The interfacial momentum transfer force comprises of force terms due to drag, turbulent diffusion, lift and a wall force:

$$\underline{M}_{ki} = \underline{M}_{ki}^{D} + \underline{M}_{ki}^{L} + \underline{M}_{ki}^{TD} + \underline{M}_{ki}^{W} \quad (5)$$

There are other forces like the virtual mass force and Basset force which are important under transient conditions but they are found to be negligible for the current class of problems (steady state bubbly). The drag force of the bubbles is given by,

$$\underline{M}_{2}^{D} = -\frac{3}{4}\alpha\rho_l \frac{C_D}{D_b}\left|\underline{\bar{v}}_R\right|\underline{\bar{v}}_R \quad (6)$$

where the drag coefficient, C_D, is given by the Ishii-Zuber correlation (1979). D_b is the Sauter mean diameter of the bubble field and the relative velocity is given by $\underline{\bar{v}}_R = \underline{\bar{v}}_2 - \underline{\bar{v}}_1$.

The wall force model accounts for the effect that keeps the centers of the bubbles no closer than approximately one bubble radius from the wall. This force is important when the lift force is present. It is given by (Antal et al., 1991):

$$\underline{M}_{2}^{W} = C_{wall}\rho_1\alpha\left|\upsilon_2 - \upsilon_1\right|^2 \underline{n}\ ,\ C_{wall} = \min\left\{0, -\left(\frac{c_{w1}}{D_b} + \frac{c_{w2}}{y_{wall}}\right)\right\} \quad (7)$$

where $\underline{n}$ and y_{wall} are the normal vector and the distance from the wall respectively. The CFX values for the coefficients are: c_{w1} = -0.01 and c_{w2} = 0.05. In a previous study (Prabhudharwadkar et al., 2009) it was found that the Antal's CFX Default coefficients work well for adiabatic bubbly flows through vertical pipe.

The turbulent diffusion force is closed using the *Lopez de Bertodano Model* (Lopez de Bertodano, 1991):

$$\underline{M}_{2}^{TD} = -C_{TD}\,\rho_1 k_1 \nabla\alpha \quad (8)$$

The turbulent diffusion coefficient used for the present calculations is C_{TD} = 0.25.

The lift force is given by (Auton (1987)):

$$\underline{M}_{2}^{L} = -C_L\,\rho_1\alpha\left(\underline{\upsilon}_2 - \underline{\bar{v}}_1\right)\times\left(\nabla\times\underline{\bar{v}}_1\right) \quad (9)$$

The lift coefficient used for the calculations is C_L = 0.1 (Lopez de Bertodano, 1991). This value is of the same order as Tomiyama's experimental value (2002) for a bubble in Couette flow, C_L = 0.288.

2.2 Interfacial heat transfer

The interface to liquid heat transfer (k=l) is expressed as,

$$q_{li} = h_{li}a_i\left(T_{sat} - T_l\right), \quad (10)$$

where, h_{li} is the heat transfer coefficient between the liquid and the interface, closed as follows,

$$h_{li} = \frac{\lambda_l}{d_s}Nu \quad (11)$$

In the above equation, λ_l is the liquid thermal conductivity and d_s is a length scale which is assumed equal to the bubble diameter. The Nusselt number (Nu) in the above closure equation is given by following expression (Ranz and Marshall, 1952):

$$Nu = 2 + 0.6\,\mathrm{Re}_b^{0.5}\,\mathrm{Pr}_l^{0.33} \quad (12)$$

Reynolds number (Re_b) used in the above closures is defined as,

$$\mathrm{Re}_b = \frac{D_b\left|\underline{\bar{v}}_R\right|}{\nu_l} \quad (13)$$

The interfacial mass transfer is given as,

$$\dot{m}_{cond,L} = \max\left(\frac{h_{li}\left(T_{sat} - T_l\right)a_i}{H_{\mathrm{lg}}}, 0\right), \quad \dot{m}_{evap,L} = \min\left(\frac{h_{li}\left(T_{sat} - T_l\right)a_i}{H_{\mathrm{lg}}}, 0\right), \quad (14)$$

where, H_{lg} is the latent heat of phase change.

2.3 Wall heat transfer

Wall heat transfer is the most important aspect of subcooled boiling as it provides the sources for energy and phase mass balance equations. Most wall heat transfer models are based on partitioning the wall heat flux into three components. These were implemented in the multidimensional CFD calculations by Kurul and Podowski (1990). The three components of the wall heat flux are –

a) Evaporation heat flux (q_e) – The part of heat flux utilized in formation of vapor at the wall,
b) Forced convection to the liquid (q_c),
c) Wall quenching by liquid phase (transient conduction) (q_q) – This accounts for the heat transfer to the subcooled liquid that replaces the detached bubble at the wall.

The wall surface is assumed to be split into two parts (A_1, A_2) each under the influence of one phase. Fraction A_2 is influenced by the vapour bubbles formed on the wall and participates in the evaporation and quenching heat transfer. Fraction A_1 is the remaining part of the wall surface, (A_1=1–A_2) and participates in the convective heat transfer to the liquid. A_1 and A_2 are related to the nucleation site density per unit wall area (n_{site}) and to the influence area of a single bubble forming at the wall nucleation site. The Kurul-Podowski model assumes, that the diameter of the bubble influence zone is twice as big as the bubble departure diameter (a = 2)

$$A_2 = \frac{\pi}{4}\left(a \cdot D_{dep}\right)^2 \cdot n_{site}\,,\; A_1 = 1 - A_2 \tag{15}$$

Evaporation Heat Flux:

The evaporation heat flux is obtained from the rate of vapor generation at the wall which is given as a product of mass of a bubble at detachment, the detachment (departure) frequency and the nucleation site density,

$$\dot{m}_e = \frac{\pi D_{dep}^3}{6}\rho_G\; f_{dep}\, n_{site} \tag{16}$$

$$q_e = \dot{m}_e h_{\mathrm{lg}} \tag{17}$$

The specification of evaporation heat flux using above equation requires closure for bubble departure diameter, bubble departure frequency and the site density. The default available model in CFX uses following closure relations:

The bubble departure diameter is given by the empirical correlation of Tolubinsky and Kostanchuk (1970), the Nucleation Site Density is obtained using the correlations of Lemmart and Chawla (1977) and the departure frequency is closed using the simplest available expression (Cole, 1960), which uses a characteristic bubble velocity (terminal velocity of bubble rise) and a characteristic bubble size (departure diameter).

The frequency of bubble departure obtained by Cole (1960) was derived under the assumption of bubble moving with terminal velocity once detached from the surface. This is a fair assumption for pool boiling scenario at low heat fluxes where bubble detachment is hydrodynamically governed, but may not be accurate for flow boiling at high heat fluxes where the thermodynamics governs the bubble growth and detachment. The CFX default closure relations are given below:

$$D_{dep} = D_{ref}\exp\left(-\left(T_{sat} - T_{liq}\right)/T_{ref}\right),\; D_{ref} = 0.6\,mm,\; T_{ref} = 45\,K \tag{18}$$

$$n_{site} = n_{ref}\,\left((T_{wall} - T_{sat})/\Delta T_{ref}\right)^{1.805}\; n_{ref} = 7.9384\times10^5\; m^{-2},\; \Delta T_{ref} = 10\,K \tag{19}$$

$$f_{dep} = \sqrt{\frac{4g\Delta\rho}{3D_{dep}\rho_{liq}}} \tag{20}$$

Quenching Heat Flux:

As mentioned previously, the quenching heat flux is the component of wall heat flux utilized to heat the cold liquid replacing the detached bubble adjacent to the heated wall. In order to evaluate this component, Mikic and Rohsenow (1969) used an analytical approach starting with transient conduction in semi-infinite medium with heated wall being the only boundary where temperature is specified.

$$\frac{\partial T(x,t)}{\partial t}=\alpha\frac{\partial^2 T(x,t)}{\partial x^2};\ T(x,0)=T_\infty, T(0,t)=T_w, T(\infty,t)=T_\infty \tag{21}$$

Kurul and Podowski (1991) made an assumption that quenching occurs between detachment of one bubble and appearance of next bubble (nucleation), and this time was assumed to be 80% of the detachment period. The final form of quenching heat transfer closure of Kurul-Podowski model is as follows:

$$h_q = 2\lambda_l\, f\sqrt{\frac{t_w}{\pi\alpha}};\ \ t_w=\frac{0.8}{f} \tag{22}$$

$$q_q = A_2\, h_q\left(T_w - T_\infty\right) \tag{23}$$

Single Phase Convection Heat Flux:

This is evaluated under the standard assumption of a logarithmic temperature profile across the turbulent boundary layer (Kader (1981), ANSYS CFX Solver Theory Guide (2006)).

$$q_{w,1ph}=\frac{\rho_l C_{p,l} u^*}{T^+}\left(T_w - T_{liq}\right) \tag{24}$$

$$\begin{aligned} &T^+ = \mathrm{Pr}_l\, y^* e^{-\Gamma} + \left(2.12\ln\left(y^*\right)+\beta\right)e^{-1/\Gamma},\\ &\beta = f(\mathrm{Pr}_l), \Gamma = f(y^*),\\ &u^* = C_\mu^{1/4} k_l^{1/2}, y^* = \rho_l u^* \Delta y/\mu_l \end{aligned} \tag{25}$$

where, Δy is the distance of the wall adjacent node from the wall, k_l is the liquid turbulence kinetic energy. In the above equation β is a function of liquid Prandtl number and Γ is a function of y^* (ANSYS CFX Solver Theory Guide (2006)).

The convective heat flux component through the liquid area fraction is thus given as,

$$q_c = A_{1f}\, h_c\left(T_w - T_{liq}\right),\ h_c=\frac{\rho_l C_{p,l} u^*}{T^+} \tag{26}$$

It should be noted here that all the wall heat flux model correlations above use a liquid temperature (T_{liq}). The single phase heat transfer correlation above uses the wall adjacent node temperature. However, in the quenching heat transfer correlation which was based on a one-dimensional model, the liquid temperature refers to the bulk mean temperature. As a good estimate, CFX approximates this temperature with the temperature at a fixed y^* (250). This is done in order to have a mesh size independent evaluation of wall heat flux partitions.

Review of the Bubble Departure Frequency and Nucleation Site Density models:

Situ et al. (2008) recently reviewed all the available departure frequency models and proposed a correlation for bubble departure frequency based on experimental data of subcooled boiling flow for wide ranges of pressure and heat flux (Basu et al. (2005), Thorncroft et al. (1998) and Situ (2004)). The departure frequency was correlated to the boiling heat flux as follows:

$$N_{fd} = 10.7 N_{qNB}^{0.634} \tag{27}$$

N_{fd} is a non-dimensional representation of frequency:

$$N_{fd}=\frac{f_{dep} D_{dep}^2}{\alpha_{Liq}}, \tag{28}$$

where, α_{Liq} is the liquid thermal diffusivity.

N_{qNB} is the dimensionless nucleate boiling heat flux obtained from Chen's correlation.

$$N_{qNB}=\frac{q''_{NB} D_{dep}}{\alpha_{Liq}\rho_g h_{fg}} \tag{29}$$

$$q''_{NB} = h_{NB}\left(T_w - T_{sat}\right) \tag{30}$$

$$h_{NB} = S(0.00122)\left[\frac{\left(\lambda^{0.79} C_p^{\ 0.45} \rho^{0.49}\right)_{Liq}}{\sigma^{0.5}\,\mu_l^{0.29} h_{fg}^{0.24} \rho_g^{0.24}}\right]\left(T_w - T_{sat}\right)^{0.24}\Delta p^{0.75} \tag{31}$$

$$\Delta p = p(T_w) - p(T_{sat}) \tag{32}$$

S is a suppression factor which is described in detail in the next section on site density (equation (41)).

However, when the frequency data of Thorncroft et al. (1998), Basu et al. (2005) and Situ (2004) was compared with the prediction of Situ et al.'s correlation and Cole's model, the accuracy of the models was found comparable as shown in the figure below (Fig. 1 (a) and (b)).

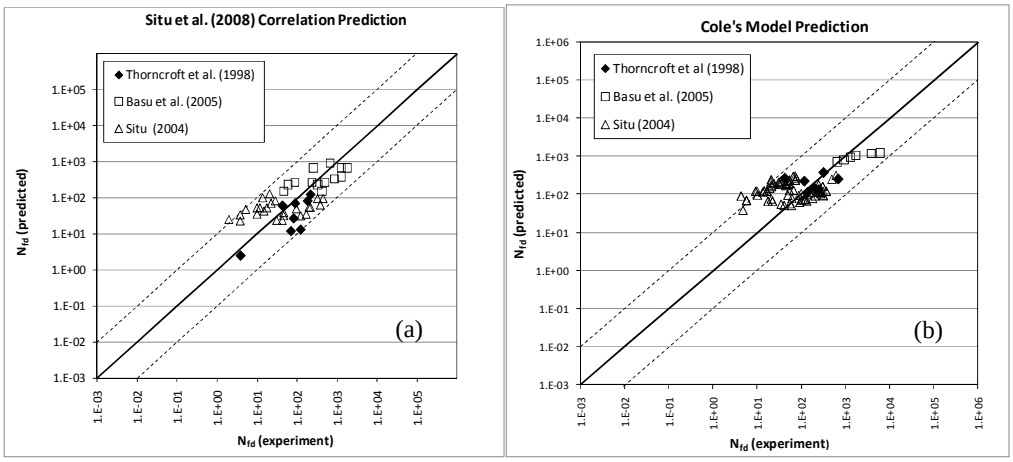

Fig. 1: Comparison of the bubble departure frequency models

The data scatter has been contained by the dotted lines in the figures above which are spaced by an order of magnitude from the correlation. The data scatter about the prediction is comparable and hence selection of the Cole's model (default CFX model) was reasonable for the present problem.

A correlation for the nucleation site density has been proposed by Hibiki and Ishii (2003) which is valid over 1-198 bar and for most practical combinations of fluid and surface material (e.g., Water-Stainless steel, Water-Copper, Water-Zr-4, R113-Nichrome etc.). This correlation is essentially an improvement of the previously established correlation of Kocamustaffaogullari and Ishii (1983) validated against water data for 0-50 bar. The Kocamustaffaogullari-Ishii (K-I) correlation relates the site density to the wall superheat as follows:

$$n^*_{site} = R_c^{*-4.4} f(\rho^*), \tag{33}$$

where,

$$n^*_{site} = n_{site} D^2_{dep} \tag{34}$$

$$R_c^* = R_C / (D_{dep}/2) \tag{35}$$

R_c is the critical radius of the surface cavity which represents a minimum cavity size which can be activated at a given wall superheat. R_c is given as,

$$R_C = \frac{2\sigma\left(1+\left(\rho_g/\rho_f\right)\right)/P}{\left(\exp\left(h_{fg}\Delta T_{sat,e}/\left(RT_gT_{sat}\right)\right)-1\right)}. \tag{36}$$

Under the following conditions:

$$\rho_g << \rho_l, \qquad h_{fg}(T_g - T_{sat})/\left(RT_gT_{sat}\right) << 1, \tag{37}$$

R_c can be simplified as,

$$R_C = 2\sigma T_{sat}/\left(\rho_g\, h_{fg}\, \Delta T_{sat,e}\right). \tag{38}$$

The density dependent parameter in equation (33) is given as,

$$f(\rho^*) = 2.157\times10^{-7}\rho^{*-3.2}\left(1+0.0049\rho^*\right)^{4.13}, \quad \rho^* = \left(\rho_l - \rho_g\right)/\rho_g \tag{39}$$

The effective wall superheat in equation (36) is usually less than the actual wall superheat. The reason for this is as follows. A bubble nucleated at the wall grows through a liquid film adjacent to the wall

where a considerably high temperature gradient exists. So, in reality, it experiences a lower mean superheat than the wall superheat. In case of pool boiling, the difference is not significant and the superheat based on the wall temperature can be taken as the effective superheat. In case of forced convective boiling, there exists a steeper temperature gradient in the near wall field due to thermal boundary layer. Hence, the effective superheat experienced by the bubble is smaller than the actual wall superheat and it is given as,

$$\Delta T_{sat,e} = S\Delta T_{sat} \text{ where, } \Delta T_{sat} = T_w - T_{sat} \tag{40}$$

The multiplier S in the above equation is the superheat suppression factor and is given as (Chen, 1966),

$$S = 1/\left(1 + 1.5\times 10^{-5}\,\mathrm{Re}_{TP}\right) \tag{41}$$

The two-phase Reynolds number is given as,

$$\mathrm{Re}_{TP} = \left[G(1-x)d_h/\mu_l\right]F^{1.25} \tag{42}$$

$$\begin{aligned} F &= 1.0 \text{ , for } X_{tt} \geq 10 \\ &= 2.35\left(0.213 + 1/X_{tt}\right)^{0.736}, \text{ for } X_{tt} < 10 \end{aligned} \tag{43}$$

The Martinelli parameter can be approximated as,

$$X_{tt} = \left(\frac{1-x}{x}\right)^{0.9}\left(\frac{\rho_g}{\rho_l}\right)^{0.5}\left(\frac{\mu_f}{\mu_g}\right)^{0.1} \tag{44}$$

Thus, equations (33)-(44) represent the complete model of Kocamustafaogullari-Ishii (1983), which has been incorporated in CFX-12 for the present study.

2.4 Turbulence Transport

The closure for the Reynolds stresses in equation (2) is based on the two-phase k-ε model developed by Lopez de Bertodano *et al.* (1994). This model assumes that the shear induced and bubble induced turbulent stresses are added together:

$$\underline{\underline{\tau}}_k^{\mathrm{Re}} = \left(\underline{\underline{\tau}}_k^{\mathrm{Re}}\right)_{SI} + \left(\underline{\underline{\tau}}_k^{\mathrm{Re}}\right)_{BI} \tag{45}$$

The resulting expression for the diffusivity of momentum (effective viscosity) of the liquid phase is:

$$\nu_{t1} = C_\mu \frac{k^2}{\varepsilon} + C_{DB}\,\alpha\, D_b \left|\underline{\upsilon}_R\right| \tag{46}$$

where, the first term on the RHS corresponds to the k-ε model for the shear induced turbulence viscosity and the second term corresponds to Sato's model (1981) for the bubble induced turbulence viscosity. The coefficient C_μ = 0.09 is the standard value according to the k-ε model. A value of 0.6 is recommended for C_{DB}. It is important to note that the k-ε model transport equations for the liquid phase are solved together with the continuity and momentum equations (Eqs. (1) and (2)). The standard coefficients of the k-ε model are left untouched.

Standard Wall Functions (Launder and Spalding (1974)) are used to model turbulence quantities near the wall which avoids need to resolve the complete boundary layer. Turbulence kinetic energy dissipation rate (epsilon) is specified using an algebraic closure assuming turbulence production due to shear is balanced by dissipation. Shear stress at the wall is connected to the velocity in the fully turbulent boundary layer (computational node next to the wall) using a logarithmic law of wall which is described in detail later.

This completes the description of the two-fluid model and all the closure relations used in the present study. The results of the comparison of two previously mentioned nucleation site density model are discussed in the subsequent section. The results reported here are restricted to the prediction of vapor void fraction distribution which of primary interest in this study.

3. RESULTS

3.1 Validation of the Heat and Mass Transfer Models

3.1.1 Subcooled boiling of R12 at 15-27 bar (Morel et al (2003))

Morel et al. (2003) performed subcooled boiling experiments in a vertical pipe of 19.2 mm internal diameter and a length of 5 m. The pipe had a heated section of 3.5 m preceded by and followed by unheated lengths of 1 m and 0.5 m respectively. The input parameters for the four tests reported were as summarized in Table 1. The liquid-vapor density ratio in these experiments corresponds to that for water-steam at 95-150 bar. Dual sensor fiber optics probes were used to measure void fraction. An experimental error of ±0.02 was reported in the void fraction measurements.

Table 1: Simulation input parameters for tests tp1 and tp6

Parameter	Test1 (Deb5)	Test2 (Deb6)	Test3 (Deb13)	Test4 (Deb10)
Mass Flux (kg/m^2)	1986	1984.9	2980.9	2027.0
Pressure (bar)	26.15	26.15	26.17	14.59
Inlet Subcooling (^{o}C)	18.12	16.11	18.12	23.24
Heat flux (W/m^2)	73.89	73.89	109.42	76.24

A 2° wedge of the pipe is used as the domain. The mesh had 20 radial and 250 axial uniformly spaced elements. Fig. 2 shows the domain and cross-section of the mesh used.

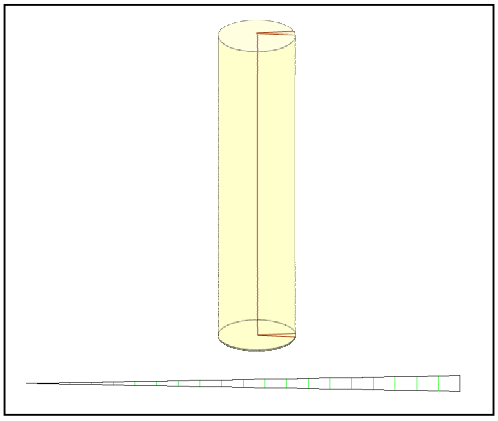

Fig. 2: Domain and Radial Mesh for R12 boiling simulation case

All the data sets include radial profiles of bubble diameter. Note that with Freon at these test pressures, the surface tension is of the order of 0.001 N/m which results into very small bubble sizes (i.e., 0.5 mm). For the CFD calculations the mean of the radial profile value is used for the bubble diameter in the bulk, whereas, the value at the wall is used as the departure bubble size (Fig. 3). An experimental error of ±12% was reported in the bubble diameter measurements. It was found during all the cases that a better match with experimental data is obtained with the coefficient of the turbulent diffusion force C_{TD} = 0.5 instead of the value obtained for adiabatic air water flows, C_{TD} = 0.25. This change may be attributed to bubble diameters in these cases which are one order of magnitude smaller than that in atmospheric air-water systems (Prabhudharwadkar et al., 2009). Therefore there are more interactions of the bubbles with smaller turbulent eddies.

Fig. 4 shows the mesh sensitivity results for Test 1 with three meshes including half and double the mesh size of the mesh size stated above. Simulations were performed using the Kocamustafaogullari-Ishii model for site density (termed as K-I Model hereafter). The mesh size dependent uncertainty in

the numerical solution was found to be lesser than the uncertainty in the measured data at the chosen mesh with 20x250 elements.

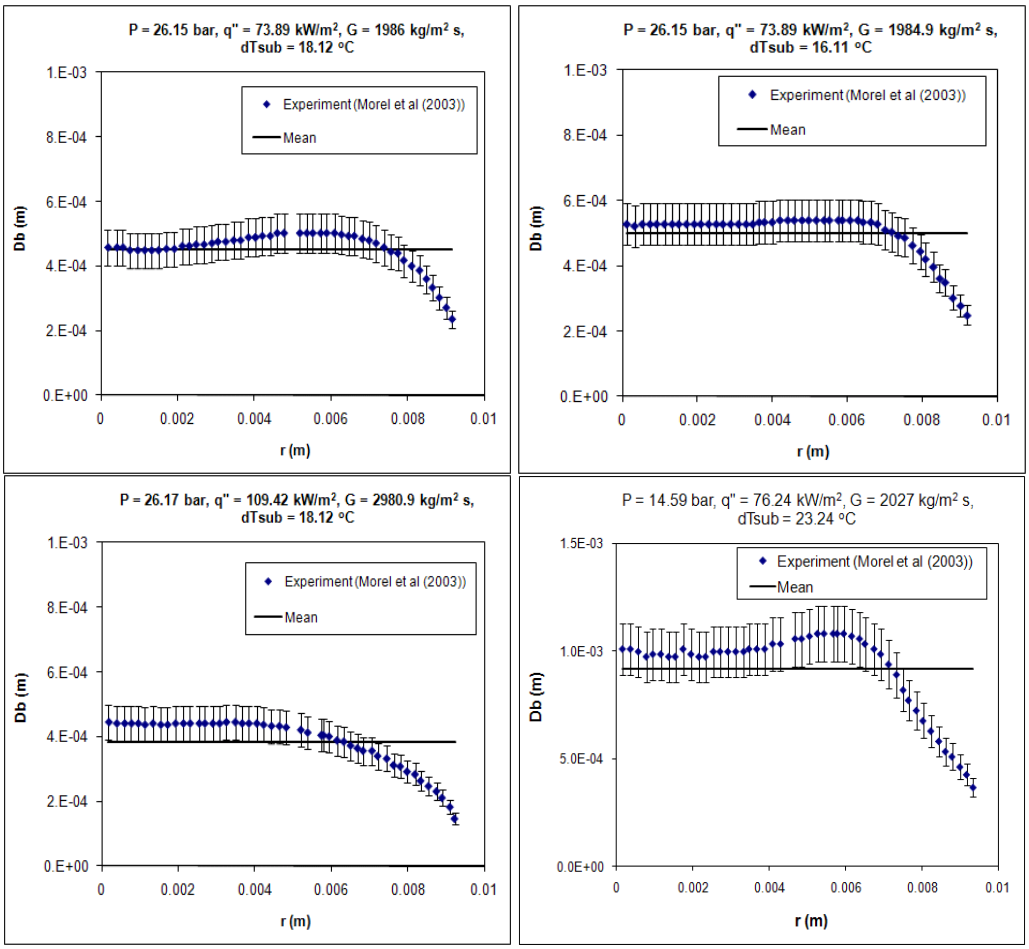

Fig.3: Bubble diameter approximation for the simulations

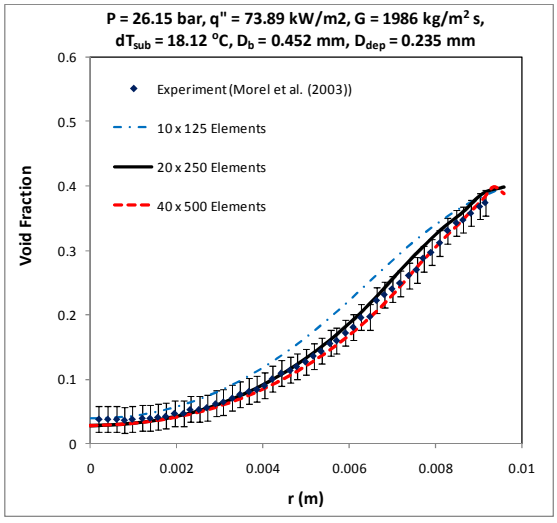

Fig. 4: Comparison of the mesh size dependent uncertainty in solution with the experimental data

Fig. 5 shows the prediction of radial variation of void fraction obtained using two different site density models. The Lemmart-Chawla (1977) correlation which is used in the Kurul-Podowski model was found to under-estimate the void fraction in all the cases. K-I model predicted the data well in all the cases. The prediction however deteriorated at low pressure data (P = 14.59 bar) and this needs further investigation.

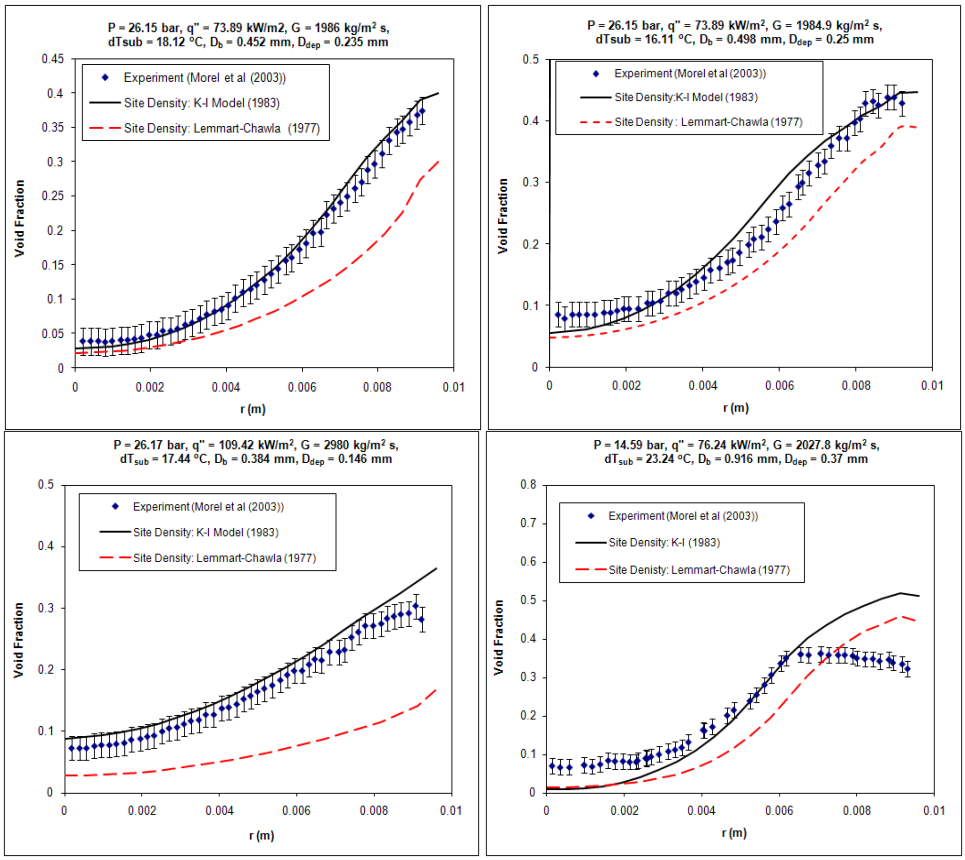

Fig. 5: Void Fraction prediction using the two Nucleation Site Density models

Fig. 6 shows the prediction of radial variation of interfacial area concentration (IAC) obtained using two different site density models. It can be seen that the IAC prediction is better with K-I site density model. However, the IAC prediction near the wall is not as accurate as that towards the pipe centre because of assumption of constant bubble size in the entire pipe. The rapid change in IAC near the wall is due to coalescence of smaller nucleated bubbles (Fig. 3) and it can be predicted using a more sophisticated approach like the one group interfacial area transport equation with a bubble coalescence model and this research is currently underway.

Fig. 7 shows the prediction of radial variation of liquid temperature obtained using two different site density models for the two test cases for which liquid temperature is reported in the reference. Lemmart-Chawla model over predicts liquid temperature near the wall and the wall superheat whereas the K-I model predicts it well near the wall with an under-prediction in wall superheat but closer prediction than the Lemmart-Chawla model.

Overall, the K-I site density model produces better results than Lemmart-Chawla model.

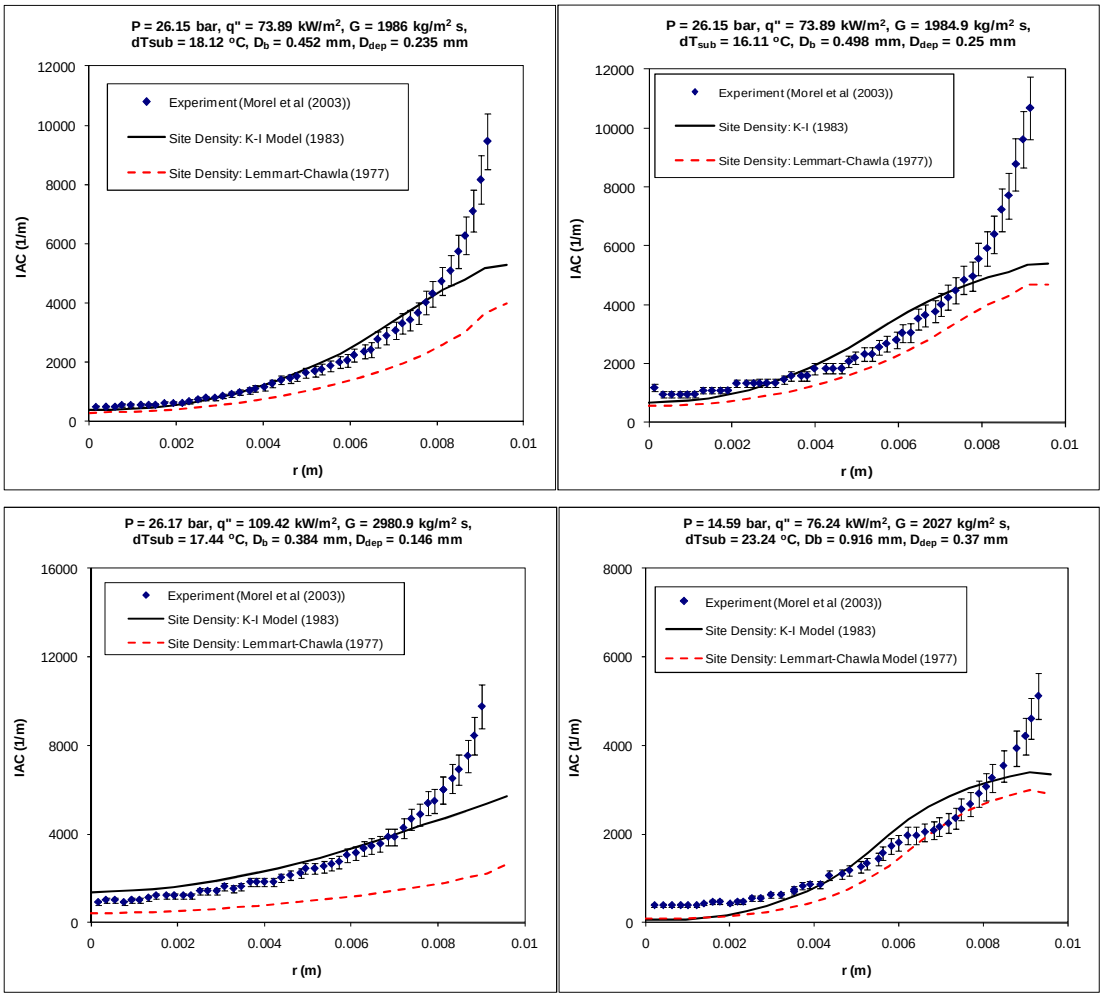

Fig. 6: Interfacial area concentration prediction using the two Nucleation Site Density models

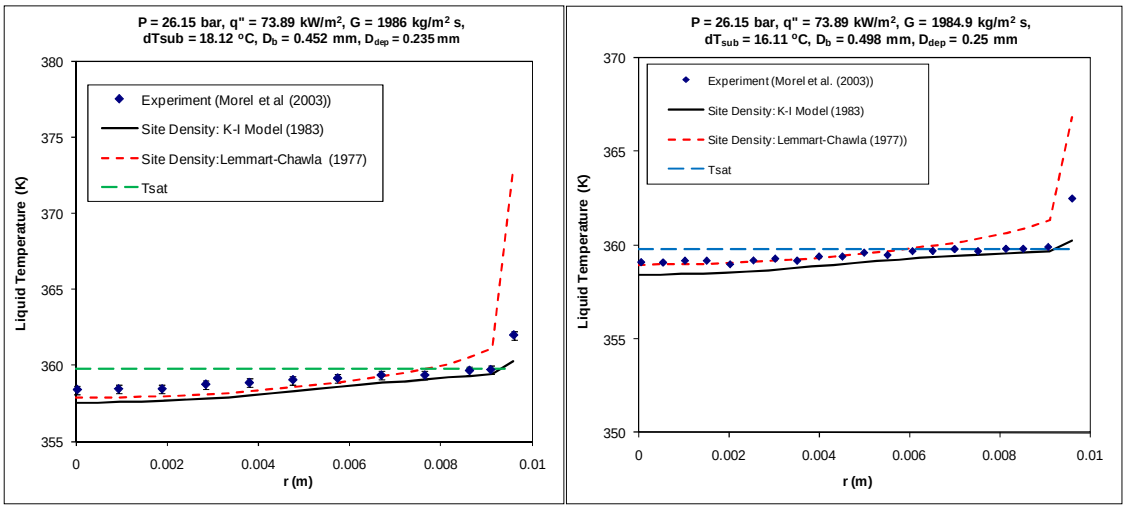

Fig. 7: Liquid temperature prediction using the two Nucleation Site Density models

3.1.2 Subcooled Boiling of R113 at 2.69 bar in an Annulus (Roy et al (2002))

Roy et al. (2002) performed subcooled boiling experiments in a vertical annulus of 15.78 mm internal diameter and 38.02 mm outer diameter. The total length of the channel was 3.66 m of which the initial 0.91 m was unheated (adiabatic). The pipe had a heated section of 2.75 m. Six experiments were reported (designated as tp1-tp6) and two of them (having minimum and maximum mass flux, tp1 and tp6) have been selected for simulation purpose here. Radial Profiles of Void Fraction were measured with a dual-sensor fiber-optic probe. An experimental error of ±2% was reported in the void fraction measurements. The input data for the two representative cases is stated in Table 2:

Table 2: Simulation input parameters for tests tp1 and tp6

Parameter	tp1	tp6
Mass Flux (kg/m^2)	568	784
Pressure (bar)	2.69	2.69
Inlet Subcooling (^{o}C)	42.7	50.2
Inner wall heat flux (W/m^2)	95000	116000

Similar to previous problem, a 2° section of the annulus is used as the domain. The mesh had 25 radial and 266 axial uniformly spaced elements. Fig. 8 shows the domain and cross-section of the mesh used.

Fig. 8: Mesh cross-section for R-113 simulations

These experiments had a characteristic near wall boundary layer of vapor (boiling layer) and the bulk of the pipe (more than 50%) had only liquid. Bubble diameter was reported for the test tp6. As the pressure was same in all the experiments and the range of other parameters was also narrow, same values were used for the other simulated case (tp1). The bubble diameter profile is shown below in Fig. 9.

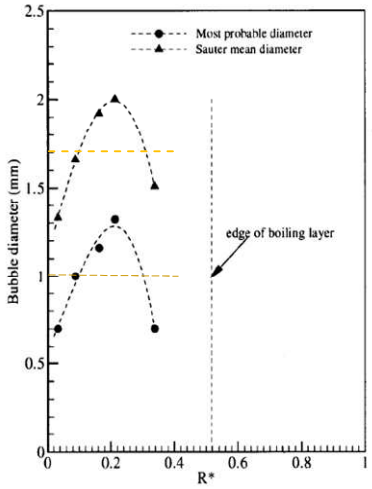

Fig. 9: Bubble diameter for case tp6

For the simulations, the bulk bubble diameter was assumed to be 1 mm and the departure bubble diameter 0.6 mm arrived at from the “most probable” diameter values reported in the experiments (Fig. 9). Simulations were also done with the Sauter mean diameter values in the bulk and at the wall; however the predictions with most probable values matched the data well. As stated earlier, the

simulations were performed with the K-I site density model only since this data set is in the pressure range for which the K-I model is already found to be best suited through previous benchmark problems. The void fraction prediction for the two cases is shown below in Fig. 10.
The width of the boiling layer was well predicted with the most probable bubble sizes; however the near wall void fraction was under-predicted in both the cases.

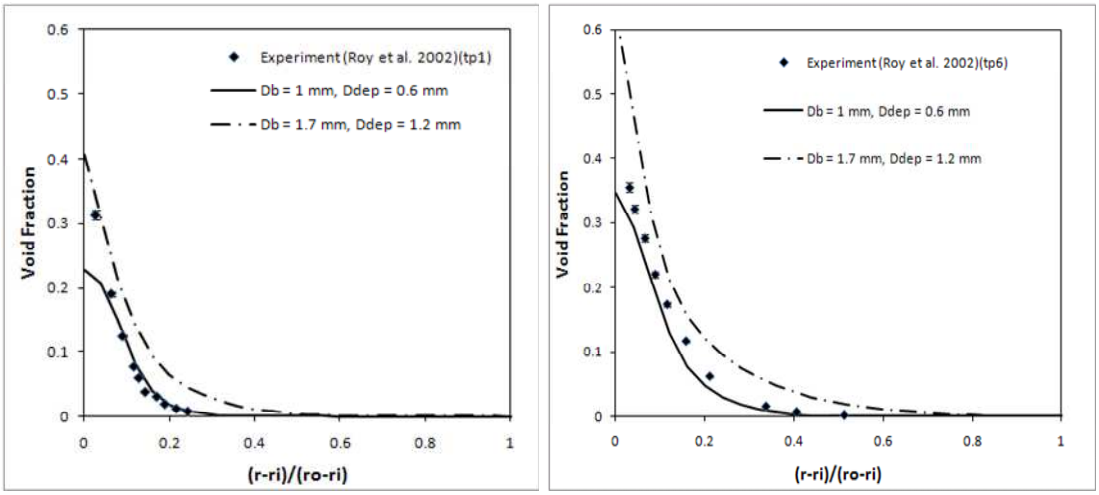

Fig. 10: Void fraction distribution prediction for tp1 and tp6 with most probable and mean diameter values

3.2 Two-phase wall function implementation

The velocity profile in the turbulent boundary layer next to the wall follows a logarithmic profile as given below:

$$U^+ = \frac{1}{\kappa}\log\left(y^+\right) + C \tag{47}$$

where, $$U^+ = \frac{U}{u_\tau}, y^+ = \frac{u_\tau y}{\nu}, u_\tau = \sqrt{\frac{\tau_w}{\rho}} \tag{48}$$

κ is the von Karman constant (= 0.41) and C is a log-layer constant (= 5.2). *U* is the velocity component tangential to the wall and *y* is the distance normal to the wall.
The above definitions are in context of single phase flow. Marie et al. (1997) performed experiments where a flat plate was placed parallel to bubbly air-water flow. Void fractions and velocity profiles were measured in the boundary layer next to the wall for different inlet concentrations of the air. It was found that the velocity profile still follows a logarithmic law-of-the-wall but with a modified slope and log layer constant. When the streamwise momentum equation for liquid phase was integrated through the fully developed two-phase boundary layer, following equation was obtained:

$$(1-\alpha)\left(\nu_L \frac{\partial U_L}{\partial y} - \langle u_L v_L \rangle\right) = u_{\tau,L}^2 - g\left(\alpha^* - \alpha_\infty\right) y_{BL} \tag{49}$$

where, $\langle u_L v_L \rangle$ is the turbulent shear stress (Reynolds stress), α^* is the average void fraction in the boundary layer and α_∞ is the average void fraction in the free stream. y_{BL} is the boundary layer thickness. The second term on the right side of the above equation represents the buoyancy due to presence of dispersed phase. Neglecting the viscous stresses, the above equation can be simplified for dilute dispersed flows as,

$$\langle u_L v_L \rangle \approx u_{\tau,L}^2 - g\left(\alpha^* - \alpha_\infty\right) y_{BL} = u_\tau^{*2} \tag{50}$$

The two-phase log layer equation proposed by Marie et al. (1997) uses u_τ^* as the velocity scale instead of u_τ in equations (47-48). When this velocity scale was used for the law of the wall it was found that

the log layer profiles for all the inlet void fraction were parallel and the log layer coefficient C increased with the inlet void fraction. Fig. 11 below shows the results obtained by Marie et al (1997) for different inlet void fractions after using a modified velocity scale.

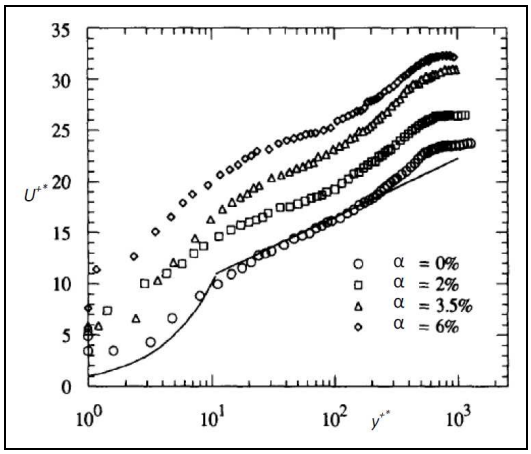

Fig.11: Log layer velocity profiles measured by Marie et al. (1997) for different air void fractions

The log layer constant for two-phase mixture, C^*, was related to the single phase C with the following relation.

$$C^* = C + y^{0+}(1/\beta - 1) - (1/\kappa)\log\beta \tag{51}$$

$$\beta = \frac{u_\tau}{u_\tau^*} \tag{52}$$

y^{0+} represents the edge of the laminar sub-layer which is usually about 11.

Based on the above model, the log layer coefficients were modified in the CFD code CFX and turbulence quantities were compared with single phase and two phase law of the wall. The above mentioned experimental benchmark of Roy et al (2002) included measurements for turbulence kinetic energy and Reynolds stress. A single phase case was first tried to validate the single phase wall function included in the CFD code CFX. Fig. 12 shows turbulence kinetic energy and Fig. 13 shows the turbulent shear stress profile for a single phase experiment reported by Roy et al (test sp1: Mass Flux = 568 kg/m^2, Pressure = 2.69 bar, Inlet Temperature = 315.85 K, Wall Heat Flux = 16 kW/m^2).
The results were satisfactory confirming adequacy of the mesh size and model accuracy for the prediction of near wall turbulence quantities.

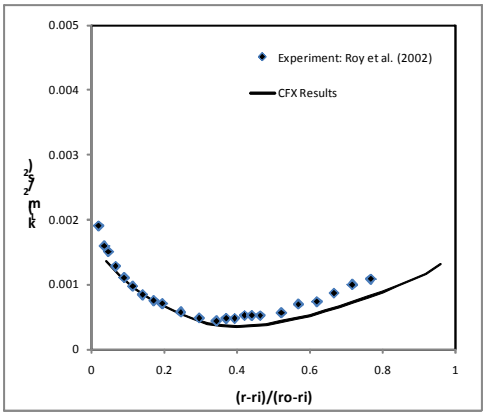

Fig. 12: Turbulence kinetic energy prediction for single phase case

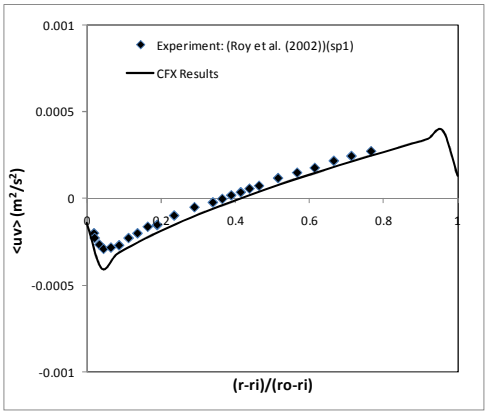

Fig. 13: Reynolds stress prediction for single phase case

The two phase log law coefficients were then implemented in CFX to compare the effective turbulence kinetic energy and turbulent stress. The effective turbulence kinetic energy superposes the shear induced and bubble induced components as follows:

$$k_{L,eff} = k_{L,SI} + k_{L,BI};\ k_{BI} = \frac{1}{4}\alpha\left|\underline{\upsilon}_R\right|^2 \tag{53}$$

Significant improvement was noticed in the prediction of the turbulence kinetic energy (Fig. 14) for both the previously reported cases especially near the boiling boundary layer edge where a single phase wall function showed a characteristic dip.

The Reynolds stress (obtained using equations (45-46)) was found to be more accurate with the modified wall law coefficients (Fig. 15).

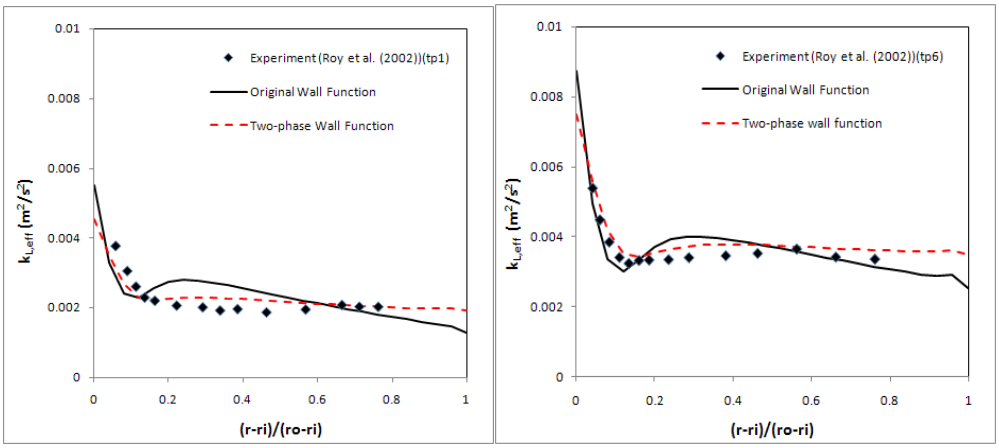

Fig. 14: Turbulence kinetic energy prediction for wall-boiling cases tp1 and tp6 of Roy et al. (2002)

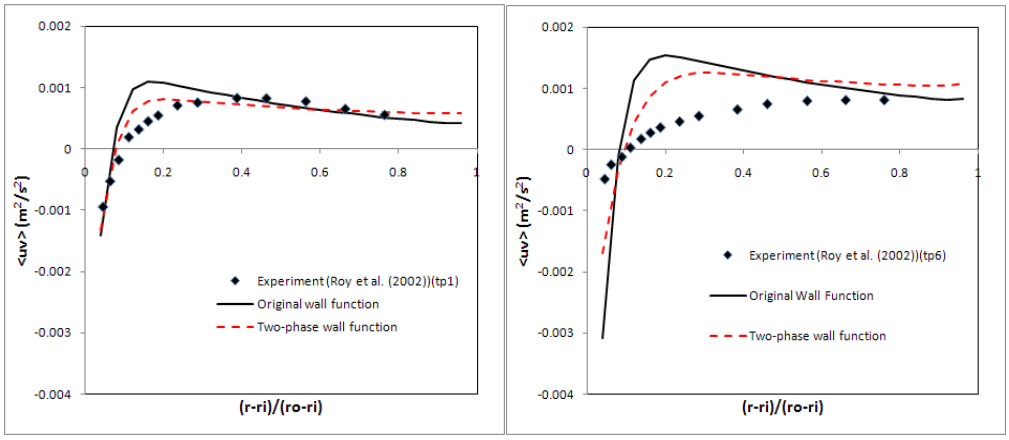

Fig. 15: Reynolds Stress prediction for wall-boiling cases tp1 and tp6 of Roy et al. (2002)

4. CONCLUSIONS

1. The heat flux splitting model for wall-boiling flows was validated using data sets where bubble diameters were known.
2. The nucleation site density model by Kocamustaffaogullari and Ishii (1983) in combination with the Bubble Departure Frequency model of Cole (1960) results in the best prediction of the data.
3. Predictions were found to deteriorate at lower pressures of the R12 data; however the results were still satisfactory.
4. Use of a modified log law coefficients based on the approach of Marie et al. (1997) improved prediction of the turbulence quantities near the wall.

REFERENCES

Anglart, H, Nylund, O., Kurul, N., Podowski, M.Z. "CFD prediction of flow and phase distribution in fuel assemblies with spacer", *Nuclear Engineering and Design*, Vol. 177, 215-228 (1997)

ANSYS CFX Solver Theory Guide, ANSYS CFX Release 11.0, (2006)

Antal, S.P., Lahey, R.T. Jr., Flaherty, J.E. "Analysis of phase distribution in fully developed laminar bubbly two-phase flow", *International Journal of Multiphase Flow*, Vol. 17, No. 5, 635-652 (1991)

Auton T. R., Hunt J. C. R. and Prud'homme M. "The force exterted on a body in inviscid unsteady non-uniform rotational flow", *Journal of Fluid Mechanics*, Vol. 197, 241–57 (1987)

Basu, N., Warrier G. R., Dhir, V.K. "Wall heat flux partitioning during subcooled flow boiling: Part II-Model validation", *Journal of Heat Transfer*, Vol. 127, 73-93 (2005)

Chen, J.C. "Correlation for boiling heat transfer to saturated fluids in convective flow", *I& EC Proc. Des. Dev.*, Vol. 5, 322–329 (1966).

Cole, R. "A Photographic Study of Pool Boiling in the Region of The Critical Heat Flux", *AIChE Journal*, Vol. 6, 533- 534 (1960).

Hibiki, T. & Ishii, M. "Active nucleation site density in boiling systems", *International Journal of Heat and Mass Transfer*, Vol. 46, 2587–2601 (2003).

Ishii, M. & Hibiki, T., "Thermo-fluid dynamics of two-phase flow", Springer (2006)

Ishii, M. & Zuber N., "Drag coefficient and relative velocity in bubbly, droplet or particulate flows", *AIChE Journal*, Vol. 25, No.5, 843-855 (1979).

Kader, B.A. "Temperature and concentration profiles in fully turbulent boundary layers", *International Journal of Heat and Mass Transfer*, Vol. 24, Issue 9, 1541-1544 (1981).

Kocamustaffaogullari G. & Ishii M. "Interfacial area and Nucleation Site Density in boiling systems", *International Journal of Heat and Mass Transfer*, Vol. 26, 1377-1397 (1983).

Kurul, N. & Podowski, M. Z., "Multidimensionnal effects in forced convection subcooled boiling", *International. Heat Transfer Conference*, Jerusalem, Vol. 1, 21-26 (1990).

Launder B.E., and Spalding D.B., "The numerical computation of turbulent flows", *Computer Methods in Applied Mechanics and Engineering*, Vol.3, pp. 269-289, 1974.

Lemmert, M., Chawla, J.M. "Influence of flow velocity on surface boiling heat transfer coefficient", Heat Transfer in Boiling, Academic Press and Hemisphere, 237–247 (1977)

Lopez de Bertodano, M. "Turbulent Bubbly Flow in a Triangular Duct", Ph. D. Thesis, Rensselaer Polytechnic Institute, Troy New York, (1991).

Lopez de Bertodano, M. A., Lahey, R. T., Jr., and Jones, O. C., "Jr. Development of a k-ε model for bubbly two-phase flow", *Journal of Fluids Engineering*, Vol. 116, 128-134 (1994).

Marie, J.L., Moursali, E., Tran-Cong, S., “Similarity law and turbulence intensity profiles in a bubbly boundary layer at low void fractions” *International Journal of Multiphase Flow*, Vol. 23, No.2, pp 227-247 (1997).

Mikic, B.B. & Rohsenow, W.M. “A new correlation of pool-boiling data including the fact of heating surface characteristics”, *Journal of Heat Transfer*, 91, 245–250, (1969).

Morel C., Yao W. & Bestion D. “Three dimensional modeling of boiling flow for the NEPTUNE code”, *Proceedings of the 10th International Topical Meeting on Nuclear Reactor Thermal Hydraulics*, Korea (2003).

Prabhudharwadkar, D.M., Bailey, C.A., Lopez de Bertodano, M.A. & Buchanan Jr., J.R. “Two-Fluid CFD model of adiabatic air-water upward bubbly flow through a vertical pipe with a One-Group Interfacial Area Transport Equation”, Paper FEDSM2009-78306, *Proceedings of the ASME 2009 Fluids Engineering Division Summer Meeting*, Vail, Colorado, USA (2009).

Ranz, W.E. & Marshall, W.R. “Evaporation from drops: Parts I&II”, *Chem. Eng. Prog.*, Vol. 48, Issue 3, 141-146 (1952)

Roy, R.P., Kang, S., Zarate, J.A., Laporta, A., “Turbulent subcooled boiling flow: Experiments and Simulations”, *Journal of Heat Transfer*, Vol. 124, 73-93 (2002).

Sato, Y., Sadatomi, M. & Sekoguchi, K. “Momentum and heat Transfer in Two-phase Bubble Flow”, *Int. J. Multiphase Flow*, Vol. 7, 179-190 (1981).

Situ, R., “Experimental and theoretical investigation of adiabatic bubbly flow and subcooled boling flow in an annulus”, Ph.D. Thesis, Purdue University, USA (2004).

Situ R., Ishii M., Hibiki, T., Tu, J.Y., Yeoh, G.H., Mori, M. “Bubble departure frequency in forced convective subcooled boiling flow”, *International J. Heat and Mass Transfer*, Vol. 51, 6268-6282 (2008).

Thorncroft, G.E., Klausner, J.F., Mei, R. “An experimental investigation of bubble growth and detachment in vertical upflow and downflow boiling”, *International Journal of Heat and Mass Transfer*, Vol. 41, 3857-3871 (1998).

Tolubinsky, V.I. & Kostanchuk, D.M. “Vapour bubbles groth rate and heat transfer intensity at subcooled water boiling”, *Proceedings of the 4th International Heat Transfer Conference*, Vol. 5, Paris (Paper No. B-2.8), (1970).

Tomiyama, A., Tamai, H., Zun, I., Hosokawa, S. Transverse migration of single bubbles in simple shear flows. Chemical Engineering Science, Vol. 57, 1849-1858 (2002)